Molecular Human Reproduction, Vol.22, No.5 pp. 613–621, 2016
Advanced Access publication on August 17, 2016 doi:10.1093/molehr/gaw046

molecular human reproduction

ORIGINAL ARTICLE

Oocyte-specific deletion of *N-WASP* does not affect oocyte polarity, but causes failure of meiosis II completion

Zhen-Bo Wang[1,2], Xue-Shan Ma[1], Meng-Wen Hu[1], Zong-Zhe Jiang[1], Tie-Gang Meng[1,2], Ming-Zhe Dong[1], Li-Hua Fan[1,2], Ying-Chun Ouyang[1], Scott B. Snapper[3,4,5], Heide Schatten[6], and Qing-Yuan Sun[1,2,*]

[1]State Key Laboratory of Stem Cell and Reproductive Biology, Institute of Zoology, Chinese Academy of Sciences, Beijing 100101, P.R. China [2]University of Chinese Academy of Sciences, Beijing 100101, P.R. China [3]Gastrointestinal Unit, Massachusetts General Hospital, Boston, MA 02114, USA [4]Center for the Study of Inflammatory Bowel Disease, Massachusetts General Hospital, Boston, MA 02114, USA [5]Department of Medicine, Harvard Medical School, Boston, MA 02115, USA [6]Department of Veterinary Pathobiology, University of Missouri, Columbia, MO 65211, USA

*Correspondence address. State Key Laboratory of Stem Cell and Reproductive Biology, Institute of Zoology, Chinese Academy of Sciences, #1 Beichen West Rd, Chaoyang, Beijing 100101, P.R. China. Tel/Fax: +8610-6480-7050; E-mail: sunqy@ioz.ac.cn

Submitted on December 12, 2015; resubmitted on May 26, 2016; accepted on June 2, 2016

STUDY QUESTION: There is an unexplored physiological role of N-WASP (neural Wiskott-Aldrich syndrome protein) in oocyte maturation that prevents completion of second meiosis.

SUMMARY ANSWER: In mice, *N-WASP* deletion did not affect oocyte polarity and asymmetric meiotic division in first meiosis, but did impair midbody formation and second meiosis completion.

WHAT IS KNOWN ALREADY: N-WASP regulates actin dynamics and participates in various cell activities through the RHO-GTPase-Arp2/3 (actin-related protein 2/3 complex) pathway, and specifically the Cdc42 (cell division cycle 42)-N-WASP-Arp2/3 pathway. Differences in the functions of Cdc42 have been obtained from *in vitro* compared to *in vivo* studies.

STUDY DESIGN, SAMPLES/MATERIALS, METHODS: By conditional knockout of N-WASP in mouse oocytes, we analyzed its *in vivo* functions by employing a variety of different methods including oocyte culture, immunofluorescent staining and live oocyte imaging. Each experiment was repeated at least three times, and data were analyzed by paired-samples *t*-test.

MAIN RESULTS AND THE ROLE OF CHANCE: Oocyte-specific deletion of N-WASP did not affect the process of oocyte maturation including spindle formation, spindle migration, polarity establishment and maintenance, and homologous chromosome or sister chromatid segregation, but caused failure of cytokinesis completion during second meiosis ($P < 0.001$ compared to control). Further analysis showed that a defective midbody may be responsible for the failure of cytokinesis completion.

LIMITATIONS, REASONS FOR CAUTION: The present study did not include a detailed analysis of the mechanisms underlying the results, which will require more extensive further investigations.

WIDER IMPLICATIONS OF THE FINDINGS: N-WASP may play an important role in mediating and co-ordinating the activity of the spindle (midbody) and actin (contractile ring constriction) when cell division occurs. The findings are important for understanding the regulation of oocyte meiosis completion and failures in this process that affect oocyte quality.

LARGE SCALE DATA: None.

STUDY FUNDING AND COMPETING INTEREST(S): This work was supported by the National Basic Research Program of China (No. 2012CB944404) and the National Natural Science Foundation of China (Nos 30930065, 31371451, 31272260 and 31530049). There are no potential conflicts of interests.

Key words: N-WASP / oocyte / polarity / meiosis II / cytokinesis

Introduction

For most mammals, oocytes are arrested in the ovaries at prophase of the first meiosis after birth, indicated by the germinal vesicle (GV) located at the center of the oocyte. Oocyte maturation includes germinal vesicle breakdown (GVBD), followed by the first asymmetric meiotic division, resulting in the formation of a mature oocyte arrested at the metaphase II (MII) stage, awaiting fertilization. Upon fertilization, the MII oocyte undergoes the second asymmetric division and emits the second polar body. During the process of oocyte maturation and fertilization, two important events take place. First, during meiosis I and meiosis II, homologous chromosomes and sister chromatids segregate, respectively, to ensure haploid gamete production. Second, the two meiotic divisions occur asymmetrically to emit small polar bodies, while maintaining almost all the cytoplasm in the egg to support early embryogenesis (Wang *et al.*, 2010, 2011; Qiao *et al.*, 2014). The asymmetric cell divisions depend on asymmetric positioning of the meiotic spindles. During oocyte maturation, the centrally organized metaphase I (MI) spindle migrates to the cortex, inducing formation of a polarized actin cap and oocyte polarity, in preparation for asymmetric division (Wang *et al.*, 2008, 2013).

The migration of the MI spindle to the cortex mainly depends on microfilament functions (Verlhac *et al.*, 2000). Two actin nucleators, Formin-2 (Dumont *et al.*, 2007; Azoury *et al.*, 2008) and Spire1/Spire2 (Pfender *et al.*, 2011), play a role in spindle migration and in polar body emission by allowing the formation of filamentous actin (Leader *et al.*, 2002). The third actin nucleator, the actin-related protein 2/3 (Arp2/3) complex, has recently been shown to regulate MI spindle migration to the cortex and polar body formation (Sun *et al.*, 2011; Yi *et al.*, 2013). Arp2/3 is widely known to nucleate the branched actin filament network by directing the formation of a new filament at a 70° branch on the side of an existing filament (Pollard and Beltzner, 2002). The Arp2/3 complex has relatively poor nucleating activity on its own (Higgs and Pollard, 1999), and the nucleation promoting factors (NPFs), which are divided into two types, function as activators for the Arp2/3 complex to nucleate branched filaments. Type I NPFs contain a characteristic VCA domain [verprolin-homology domain (also known as WH2), the cofilin-homology domain (also known as central domain) and the acidic domain] composed of three conserved motifs that allow for the binding of G-actin (through the V motif) and ARP2/3 (through the CA motif). Type I NPFs include the Wiskott-Aldrich syndrome protein (WASP) family verprolin-homologous protein (WAVE; also known as SCAR), WASP, neural WASP (N-WASP), WASP and SCAR homolog (WASH) and junction-mediating and regulatory protein (Rotty *et al.*, 2013). Type II NPFs such as cortactin lack complete VCA domains, but they have acidic domains at their amino terminus that bind the ARP2/3 complex and tandem repeat domains that bind F-actin. WASP and N-WASP remain inactive by auto-inhibition through intramolecular association between their VCA domain and GTPase-binding domain, and their activation depends on Cdc42 (cell division cycle 42) binding (Higgs and Pollard, 2001; Padrick and Rosen, 2010).

N-WASP was first discovered in brain to regulate the cortical cytoskeletal rearrangement (Miki *et al.*, 1996). N-WASP regulates actin dynamics and participates in various kinds of cell activities through the RHO-GTPase -Arp2/3 pathway, especially the Cdc42-N-WASP-Arp2/3 pathway. Cdc42 regulates dendritic spine morphogenesis and synapse formation via its effector N-WASP, activating the Arp2/3 complex (Wegner *et al.*, 2008; Rocca and Hanley, 2015). In neuroendocrine cells, the Cdc42-N-WASP-Arp2/3 pathway mediates exocytosis by regulating actin reorganization (Gasman *et al.*, 2004). In the regulation of cell migration, the Cdc42-N-WASP-Arp2/3 pathway regulates

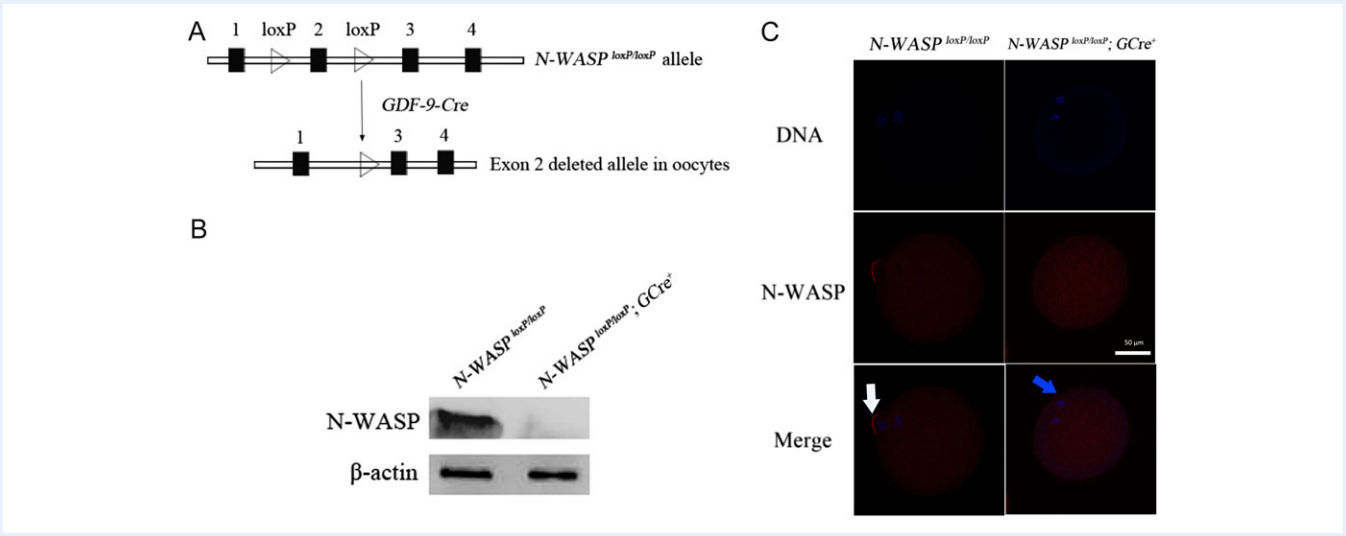

Figure 1 Specific deletion of *N-WASP* in mouse oocyte. (**A**) Schematic representation of *N-WASP* exon 2 deletion by *GDF9*-Cre (Causes recombination)-mediated recombinase in oocytes. (**B**) Western blots showing the absence of N-WASP in oocytes of *N-WASP*$^{loxP/loxP}$; *GCre*$^{+}$(*GDF9-Cre*$^{+}$) mice. Proteins from a total of 150 GV (germinal vesical) oocytes were loaded for each sample. β-Actin levels were used as internal controls. Experiments were repeated three times and a representative image is shown. (**C**) Absence of N-WASP in *N-WASP*$^{loxP/loxP}$; *GCre*$^{+}$ oocyte during Meiosis I. Oocytes undergoing maturation (Meiosis I) were fixed and stained with anti-N-WASP antibody (red) and counterstained with DAPI to visualize DNA (blue). Bar = 50 μm. Experiments were repeated at least three times and representative images are shown.

lamellipodia protrusion (Nakagawa *et al.*, 2001) or filopodium formation (Martinez-Quiles *et al.*, 2001) and invadopodium formation in cancer cells (Yamaguchi *et al.*, 2005; Beaty and Condeelis, 2014).

A recent study showed that knockdown of N-WASP by morpholino or dominant-negative mutant affected the localization of Arp2/3 and anchoring of the MII spindle at the cortex (Yi *et al.*, 2013). However, our recent study by conditional knockout showed that Cdc42, an important element in the Cdc42-N-WASP-Arp2/3 pathway, is not required for MI spindle migration, but for the first polar body emission *in vivo* (Wang *et al.*, 2013). Considering the difference between the roles of Cdc42 obtained from knockdown experiments *in vitro* and knockout experiments *in vivo* (Wang *et al.*, 2013), we further investigated the *in vivo* role of N-WASP in mouse oocytes. We found that oocyte-specific deletion of *N-WASP* did not affect the process of oocyte maturation including spindle formation, migration, polarity establishment and maintenance, and homologous chromosome or sister chromatid segregation, but caused failure of cytokinesis completion during the second meiosis. Further analysis showed that a defective midbody may be responsible for the failure of cytokinesis completion.

Materials and Methods

All chemicals were purchased from Sigma (St. Louis, MO, USA) unless otherwise indicated.

Mice

Homozygous *N-WASP*$^{loxP/loxP}$ mice (129 and C57BL/6 J mixed background) were intercrossed with *GDF9-Cre* transgenic mice (C57BL/6 backround) to generate *N-WASP*$^{loxP/loxP}$; *GCre*$^{+}$ animals. Control mice were littermates possessing two *loxP* flanked alleles without Cre (*N-WASP*$^{loxP/loxP}$). Mice were maintained in alternating 12-h light/dark cycles. Animal care and use were carried out in accordance with the Animal Research Committee guidelines of the Institute of Zoology, Chinese Academy of Sciences, China.

Oocyte collection, culture and pathenogenetic activation

Four-to-eight-week-old female mice were used in the experiments. For *in vitro* maturation, GV oocytes were collected and cultured in M16 medium under liquid paraffin oil at 37°C in an atmosphere of 5% CO_2 in air. To obtain MII oocytes, mice were induced to superovulate by i.p. injection of eight IU PMSG followed 48 h later by injection of eight IU hCG. Fourteen to 15 h after hCG injection, mice were sacrificed and the oviductal ampullae were broken to release the cumulus–oocyte complexes. MII oocytes were freed of cumulus cells by exposure to 300 μg/ml hyaluronidase. Oocytes were collected for immunofluorescent staining, microinjection or immunoblot analysis. For pathenogenetic activation, the ovulated MII oocytes were cultured in Ca^{2+}, Mg^{2+}-free CZB medium supplemented with 10 mM $SrCl_2$.

Microinjection and live oocyte imaging

Microinjection of Alexa 488-phalloidine (Invitrogen, Carlsbad, CA, USA) into GV oocytes was performed using a Nikon Diaphot ECLIPSE TE 300 (Nikon UK Ltd, Kingston upon Thames, Surrey, UK) inverted microscope equipped with Narishige MM0202N hydraulic three-dimensional micromanipulators (Narishige, Inc., Sea Cliff, NY, USA) and completed within 30 minutes. After 1–2 h of culture, the microinjected oocytes were used for live oocyte imaging on a PerkinElmer precisely Ultra VIEW VOX confocal Imaging System (PerkinElmer, Waltham, MA,USA).

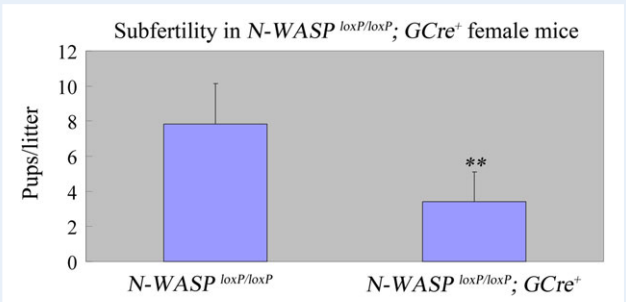

Figure 2 Oocyte-specific deletion of *N-WASP* causes female subfertility in mice. Comparison of the average number of pups per litter per female mice during a period of 6 months between *N-WASP*$^{loxP/loxP}$; *GCre*$^{+}$ (n = 3, 2.3 ± 1.7) and *N-WASP*$^{loxP/loxP}$ (n = 3, 7.8 ± 3.4) mice. $^{**}P < 0.01$. The data are mean ± SEM. The data were analyzed by paired-samples t-test.

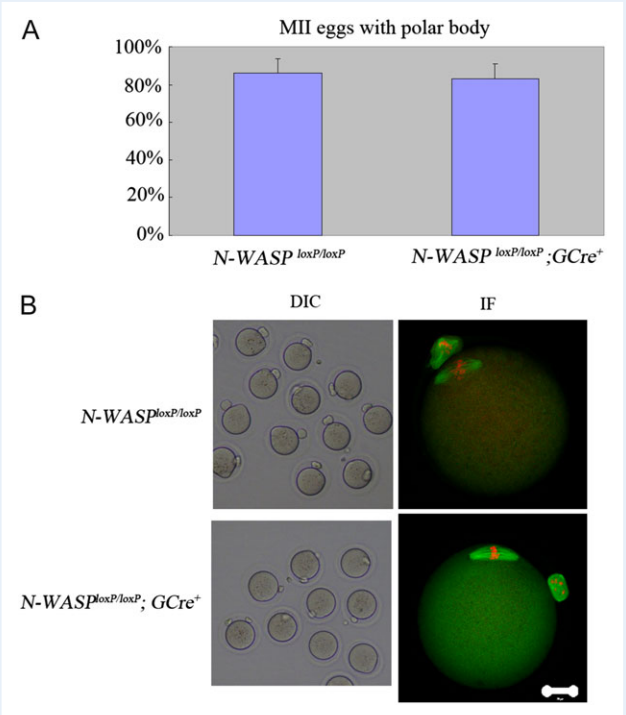

Figure 3 Normal MII oocytes superovulated from *N-WASP*$^{loxP/loxP}$; *GCre*$^{+}$ mouse. (**A**) Comparison of the rates of MII oocytes with the first polar body from superovulated *N-WASP*$^{loxP/loxP}$ female (n = 3, 86.2% ± 7.7%) and *N-WASP*$^{loxP/loxP}$; *GCre*$^{+}$ female (n = 3, 83.0% ± 8.0%). The data are mean ± SEM. (**B**) DIC (differential interference contrast), representative images of ovulated oocytes are presented (×20). Ovulated oocytes were fixed and stained with anti-α-tubulin-fluorescein isothiocyanate antibody (green) and counterstained with the fluorescent dye PI to visualize DNA (red). Bar = 50 μm for the two images in "IF" column. Experiments were repeated at least three times and representative images are shown.

Immunofluorescence and confocal microscopy

For single staining of α-tubulin or actin, oocytes were fixed in 4% paraformaldehyde in phosphate-buffered saline (PBS, pH 7.4) for at least 30 min at room temperature. After being permeabilized with 0.5% Triton X-100 at room temperature for 20 min, oocytes were blocked in 1% bovine serum albumin-supplemented PBS for 1 h and incubated overnight at 4°C with 1:200 anti-α-tubulin-fluorescein isothiocyanate antibody or 1:200 Alexa 488-phalloidine or 1:100 anti-N-WASP antibody. After three washes in PBS containing 0.1% Tween-20 and 0.01% Triton X-100, the oocytes were stained with propidium iodide (PI) (10 μg/ml in PBS) or 4′,6-diamidino-2-phenylindole (DAPI, 10 μg/ml in PBS). Then, the oocytes were mounted on glass slides and examined with a confocal laser scanning microscope (Zeiss LSM 780, Berlin, Germany).

Immunoblot analysis

Samples each containing 150 mouse oocytes were collected in sodium dodecyl sulfate (SDS) sample buffer and heated for 5 min at 100°C. The proteins were separated by SDS-polyacrylamide gel electrophoresis and then electrically transferred to polyvinylidene fluoride membranes. After transfer, membranes were blocked in TBST buffer (TBS containing 0.1% Tween-20) containing 5% skimmed milk for 2 h, followed by incubation overnight at 4°C with 1:1000 rabbit monoclonal anti-N-WASP antibody (Cell Signaling Technology, Boston, MA, USA) and 1:1000 mouse monoclonal anti-β-actin antibody (Proteintech, Chicago, IL, USA). After three washes 10 min each in TBST, the membranes were incubated for 1 h at 37°C with 1:1000 horseradish peroxidase-conjugated goat anti-rabbit immunoglobulin G. Finally, the membranes were processed using the enhanced chemiluminescence detection system (Amersham, Piscataway, NJ, USA).

Statistics

All percentages from at least three repeated experiments were expressed as mean ± SEM. Data were analyzed by paired-samples *t*-test. $P < 0.05$ was considered statistically significant. The statistical software package SPSS was used (IBM, Armonk, New York, USA).

Results

Generation of mutant mice with oocyte-specific deletion of N-WASP

To study the functions of N-WASP during mouse oocyte meiotic maturation *in vivo*, we generated mutant mice in which the *N-WASP* gene was deleted in oocytes of primordial follicles and follicles at later stages. The mutant mice (referred to as *N-WASP*$^{loxP/loxP}$; *GCre*$^{+}$ mice) were generated by crossing *N-WASP*$^{loxP/loxP}$ mice (Cotta-de-Almeida *et al.*, 2007) with transgenic mice expressing growth differentiation factor 9 (*GDF9*)-promoter-mediated Cre recombinase (Hu *et al.*, 2014; Jiang *et al.*, 2014) (Fig. 1A). By Western blot and immuno-staining, we found that the expression of N-WASP protein was absent in oocytes

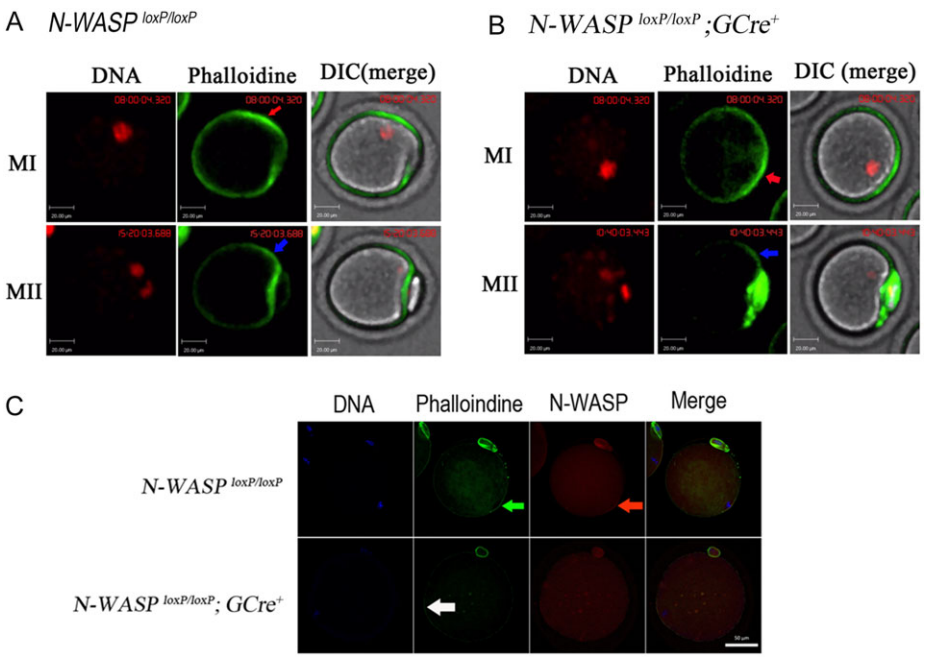

Figure 4 *N-WASP* deletion does not affect actin cap formation. Red arrow indicates the actin cap in *N-WASP*$^{loxP/loxP}$ oocytes; blue arrow indicates the actin cap in *N-WASP*$^{loxP/loxP}$; *GCre*$^{+}$ oocytes. For A and B, chromosomes are stained in blue by Hoechst 33342 (2 ng/ml in M16 medium) and the color was changed into red. Alexa 488-phalloidine was microinjected into GV oocytes to show the actin dynamics during oocyte maturation. Bar = 20 μM. (**A**) The dynamics of Alexa 488-phalloidine during *N-WASP*$^{loxP/loxP}$ oocyte maturation. MI, metaphase I; MII, metaphase II. (**B**) The dynamics of Alexa 488- phalloidine during *N-WASP*$^{loxP/loxP}$; *GCre*$^{+}$ maturation. MI, metaphase I; MII, metaphase II. (**C**) Normal actin cap and absence of N-WASP in *N-WASP*$^{loxP/loxP}$; *GCre*$^{+}$ MII oocytes. Oocytes were stained with anti-N-WASP antibody (red), Alexa 488-phalloidine (green) and DAPI (10 μg/ml, blue), and viewed with confocal microscopy. Green arrow indicates the actin cap in *N-WASP*$^{loxP/loxP}$ MII oocytes; red arrow indicates N-WASP in *N-WASP*$^{loxP/loxP}$ MII oocytes; white arrow indicates the actin cap in *WASP*$^{loxP/loxP}$; *GCre*$^{+}$ MII oocytes. Bar = 50 μM.

of mutant mice (Fig. 1B and C), showing successful deletion of the *N-WASP* gene from oocytes.

Subfertility in *N-WASP*$^{loxP/loxP}$; *GCre*$^{+}$ mice

To investigate the effect of *N*-WASP deletion on female fertility, breeding assay was carried out by mating *N-WASP*$^{flox/flox}$ or *N-WASP*$^{flox/flox}$; *GCre*$^{+}$ mice with males of proven fertility for 6 months. As shown in Fig. 2, female *N-WASP; GCre*$^{+}$ mice were severely subfertile and gave birth to ~70% fewer pups compared to control mice (mean ± SEM: 2.3 ± 1.7 versus 7.8 ± 3.4).

Normal oocyte maturation in *N-WASP*$^{loxP/loxP}$; *GCre*$^{+}$ mice

To investigate the possible reasons for the subfertility, we first performed superovulation experiments. There was no difference between the numbers of ovulated oocytes from *N-WASP*$^{loxP/loxP}$ and *N-WASP*$^{loxP/loxP}$; *GCre*$^{+}$ ovaries (24.1 ± 4.2 versus 26.4 ± 5.1), and the rates of the ovulated eggs with the first polar body were similar (Fig. 3A). The oocytes ovulated from both *N-WASP*$^{loxP/loxP}$ and *N-WASP*$^{loxP/loxP}$; *GCre*$^{+}$ ovaries displayed normal features of mature MII eggs, with the first polar body and a typical MII spindle (Fig. 3B). It appeared that the oocytes from mutant ovaries underwent maturation; we then tracked the process of oocyte maturation to determine whether maturational defects were present. As an *in vitro* study has reported that N-WASP is required for actin cap formation in mouse oocytes, it was of interest to explore if the subfertility originated from polarity impairment although the process of oocyte maturation appears normal. We carried out live oocyte imaging experiments in which we monitored chromosome and actin dynamics during oocyte maturation. As shown in Fig. 4A (also see Supplementary Movie 1), oocytes from *N-WASP*$^{loxP/loxP}$ ovaries underwent a normal meiotic maturation process. At 8 h of GVBD, the chromosomes had attached to the cortex and induced the formation of the actin cap (Fig. 4A, MI, red arrow). The homologous chromosomes then segregated and the first polar body was emitted. After polar body formation, the MII chromosomes underneath the membrane and oocyte polarity (actin cap) were maintained. Thus, the *N-WASP*$^{loxP/loxP}$; *GCre*$^{+}$ oocytes underwent maturation normally and similar to the control oocytes (Fig. 4B and Supplementary Movie 2). We further carried out immunofluorescent experiments to show that the actin cap remained intact in the fixed *N-WASP*$^{loxP/loxP}$; *GCre*$^{+}$ MII oocytes (Fig. 4C, blue arrow; Supplementary Fig. S1).

N-WASP deletion disrupts cytokinesis during second meiosis

To explore the reason underlying the subfertility, we continued to analyze whether the fertilization process (the second meiosis) was affected. Eighteen hours after mating with male mice with proven fertility, the *N-WASP*$^{loxP/loxP}$ and *N-WASP*$^{loxP/loxP}$; *GCre*$^{+}$ females were sacrificed to obtain the one-cell embryos. The control embryos showed two normal pronuclei (129/135) (Fig. 5A, red arrow), while most of the embryos from *N-WASP*$^{loxP/loxP}$; *GCre*$^{+}$ females failed to form the two pronuclei (115/146). By immunofluorescent staining, we found several defective phenotypes in pronucleus formation in embryos from *N-WASP*$^{loxP/loxP}$; *GCre*$^{+}$ females (Fig. 5B), which are listed below: embryos with pairs of sister chromatids (MII) [(21/75) versus (5/45, control)]; embryos with segregated sister chromatids (Anaphase II) but without pronucleus [(6/75) versus (2/45, control)]; embryos with one pronucleus [(19/75) versus (3/45, control)] and embryos with two pronuclei [(24/75) versus (35/45, control)].

Next we carried out parthenogenetic activation experiments to explore the possible mechanism(s) underlying the phenotypes. First, we analyzed the rates of normal single pronuclei. As shown in Fig. 6A, at 5 h of activation, a single pronucleus formed in most *N-WASP*$^{loxP/loxP}$

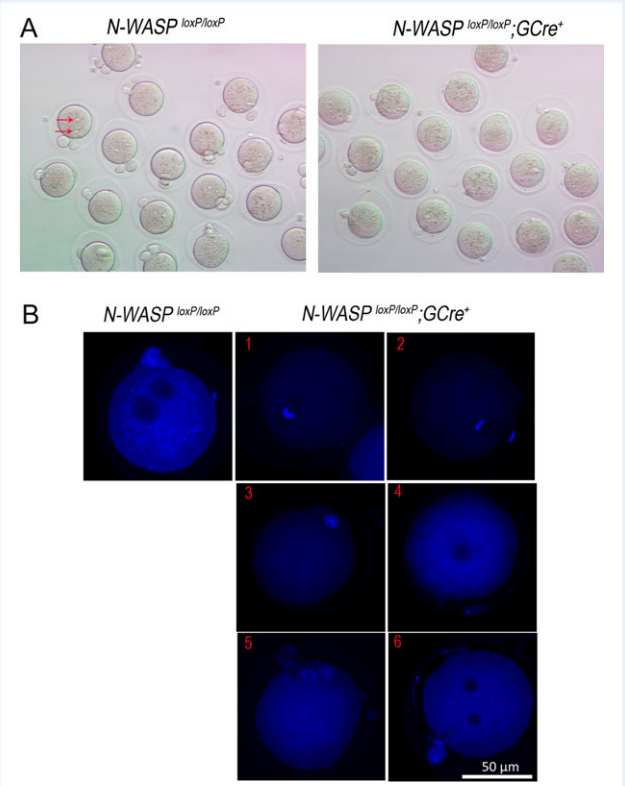

Figure 5 Disrupted pronuleus formation in embryos from *N-WASP*$^{loxP/loxP}$; *GCre*$^{+}$ females. The female mice were injected with eight IU PMSG (pregnant mare's serum gonadotrophin) followed 48 h later by injection of eight IU hCG, and then mated with male mice with proven fertility. Eighteen hours after hCG injection, mice were sacrificed and the oviductal ampullae were broken to release the cumulus-enclosed embryos. The embryos were freed of cumulus cells by exposure to 300 μg/ml hyaluronidase. (**A**) DIC images for embryos from both groups (×10). Red arrows indicate the two normal pronuclei in control embryos. Experiments were repeated at least three times (two female mice per group each time), and representative images are shown. (**B**) Confocal images of embryos from *N-WASP*$^{loxP/loxP}$ and *N-WASP*$^{loxP/loxP}$; *GCre*$^{+}$ females. 1, indicates the embryos with pairs of sister chromatids (failed fertilization). 2, indicates the embryos with segregated sister chromatids but without pronucleus. 3 and 4, indicate the embryos with one pronucleus; the pronucleus in 3 has some nucleoli. 5 and 6, indicate the embryos with two pronuclei; the pronucleus in 5 has some nucleoli. The experiments were repeated at least three times and the representative images were shown. Bar = 50 μm.

eggs (97.4 ± 0.4%), while the rate of single pronuclei became sharply reduced in *N-WASP*$^{loxP/loxP}$; *GCre*$^{+}$ eggs (16.7 ± 2.7%). The status of pronuclei in eggs was examined based on immunofluorescent staining, as shown in Fig. 6B. Compared with normal single pronuclei in *N-WASP*$^{loxP/loxP}$ eggs, several defects existed in *N-WASP*$^{loxP/loxP}$; *GCre*$^{+}$ eggs (Fig. 6B), including: an egg with two sets of chromosomes, without a pronucleus; an egg with one pronucleus and a set of chromosomes; an egg with two pronuclei of different sizes and an egg with two equal-sized pronuclei. Accordingly, the differential interference contrast (DIC) images in Fig. 6C also provide indications of the defects in the *N-WASP*$^{loxP/loxP}$; *GCre*$^{+}$ eggs at 5 h of parthenogenetic activation.

To explore the events occurring during the parthenogenetic activation process, we carried out live oocyte imaging experiments. As shown in Fig. 7A, sister chromatids separated at the expected time at about 1 h of activation in *N-WASP*$^{loxP/loxP}$ oocytes, and then oocytes emitted the second polar body (Fig. 7A, 1 h 20 min, 2 h; also see Supplementary Movie 3). For *N-WASP*$^{loxP/loxP}$; *GCre*$^{+}$ oocytes, sister chromatids separated normally and at the expected time (Fig. 7B, 1 h; also see Supplementary Movie 4), and second polar body emission was initiated (membrane protrusion) (Fig. 7B, 2 h, 2 h 20 min; also see Supplementary Movie 4) but eventually failed (Fig. 7B, 3 h 40 min; also see Supplementary Movie 4). To determine the possible reason, we fixed both the *N-WASP*$^{loxP/loxP}$ and *N-WASP*$^{loxP/loxP}$; *GCre*$^{+}$ MII oocytes undergoing MII exit and observed some *N-WASP*$^{loxP/loxP}$ MII oocytes emitting the second polar body. As shown in Fig. 7C, we could see the normal anaphase spindle and the midbody (blue arrow) in control oocytes, while the midbody was abnormal in *N-WASP*$^{loxP/loxP}$; *GCre*$^{+}$ oocytes, although the MII spindle looked intact (Fig. 3B). Surprisingly, we observed an impaired (non-constricted) contractile ring in *N-WASP*$^{loxP/loxP}$; *GCre*$^{+}$ MII oocytes undergoing MII exit (32/46) (Fig. 7D), which may link the abnormal midbody to the failed MII exit phenotype in these oocytes.

Discussion

In this study, we explored the functions of *N-WASP* in mouse oocyte maturation *in vivo* by conditional knockout technology. Oocyte-specific deletion of *N-WASP* does not affect the process of mouse oocyte maturation, including normal spindle formation, homologous chromosome segregation, polarity formation and first polar body emission. However, *N-WASP* deletion inhibited the second polar body emission by impairing the midbody formation and cytokinesis completion during the second meiosis.

N-WASP is not required for oocyte maturation *in vivo*

In various kinds of cell types, N-WASP functions play a role in a conserved Cdc42-N-WASP-Arp2/3 pathway to regulate actin filament dynamics, and this pathway has been observed in mouse oocytes but it is not understood well (Yi *et al.*, 2011; Dehapiot *et al.*, 2013). In a recent study, we found that oocyte-specific deletion of *Cdc42* resulted in female infertility, and further investigation showed that Cdc42 deletion inhibited first polar body emission by inhibiting the formation of the polarized actin cap and cytokinesis, but it had little effect on spindle

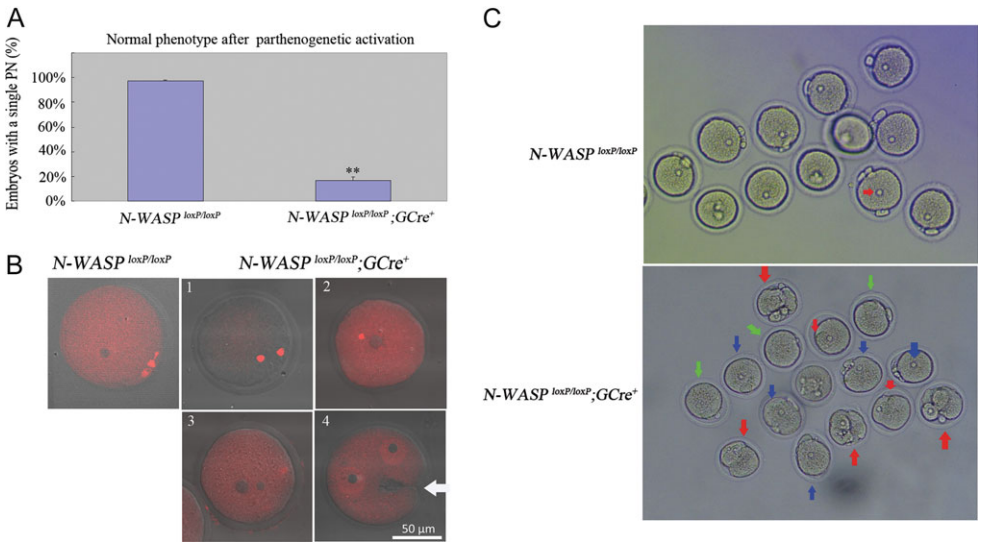

Figure 6 *N-WASP* deletion results in defects of meiosis II. (**A**) Decreased normal phenotype (embryos with normal morphology and with single pronuclear formation) for *N-WASP*$^{loxP/loxP}$; *GCre*$^{+}$ MII eggs 5 h after parthenogenetic activation. $^{**}P < 0.001$. The data were analyzed by paired-samples *t*-test. (**B**) Typical images of *N-WASP*$^{loxP/loxP}$ and *N-WASP*$^{loxP/loxP}$; *GCre*$^{+}$ MII eggs 5 h of parthenogenetic activation. Red, DNA. White arrow indicates furrow between the two pronuclei. 1, representative image of the egg with two sets of chromosomes, without pronucleus; 2, typical image of an egg with one pronucleus and a set of chromosomes; 3, representative image of an egg with two different-size pronuclei; 4, typical image of an egg with two equal-sized pronuclei. The experiments were repeated at least three times. Bar = 50 μm. (**C**) DIC images show the *N-WASP*$^{loxP/loxP}$ and *N-WASP*$^{loxP/loxP}$; *GCre*$^{+}$ MII eggs 5 h of parthenogenetic activation (×10). For *N-WASP*$^{loxP/loxP}$, red arrow indicates the normal single pronucleus. For *N-WASP*$^{loxP/loxP}$; *GCre*$^{+}$, blue arrow indicates the eggs with normal pronucleus, green arrow indicates the eggs without pronucleus and orange arrow indicates the eggs with furrow.

organization, spindle migration to the cortex or homologous chromosome segregation during first meiosis (Wang *et al.*, 2013). Interestingly, Cdc42 displays similar and important functions during the first polar body emission in *Xenopus* oocytes (Ma *et al.* 2006). In this study, we showed that oocyte-specific deletion of *N-WASP* caused female subfertility, but reduced fertility was not rooted from the first meiosis, because N-WASP deletion had little effect on the process of oocyte meiotic maturation as well as the first polar body emission (Figs 2 and 3), in accordance with the *in vitro* results reported recently (Dehapiot *et al.*, 2013). Compared with the *in vivo* function of Cdc42 that is required for actin cap formation through the Arp2/3 complex, it is unexpected that oocyte-specific *N-WASP* deletion does not inhibit actin cap formation and the first polar body emission (Figs 3 and 4). Strikingly, the actin cap is normal in *N-WASP*-deleted MII oocytes, and the MII spindle attaches to the cortex normally (Fig. 4). However, it is reported that *in vitro* inhibition of N-WASP (Yi *et al.*, 2011; Dehapiot *et al.*, 2013) or the Arp2/3 complex (Yi *et al.*, 2011) in MII oocytes resulted in compromised polarity and detachment of MII spindle/chromosomes from the cortex. As described previously, like N-WASP, the type I NPFs all have the domains for binding of G-actin or the Arp2/3 complex, and could function in actin dynamics (Padrick and Rosen, 2010). Thus, some other WASP protein or proteins might replace N-

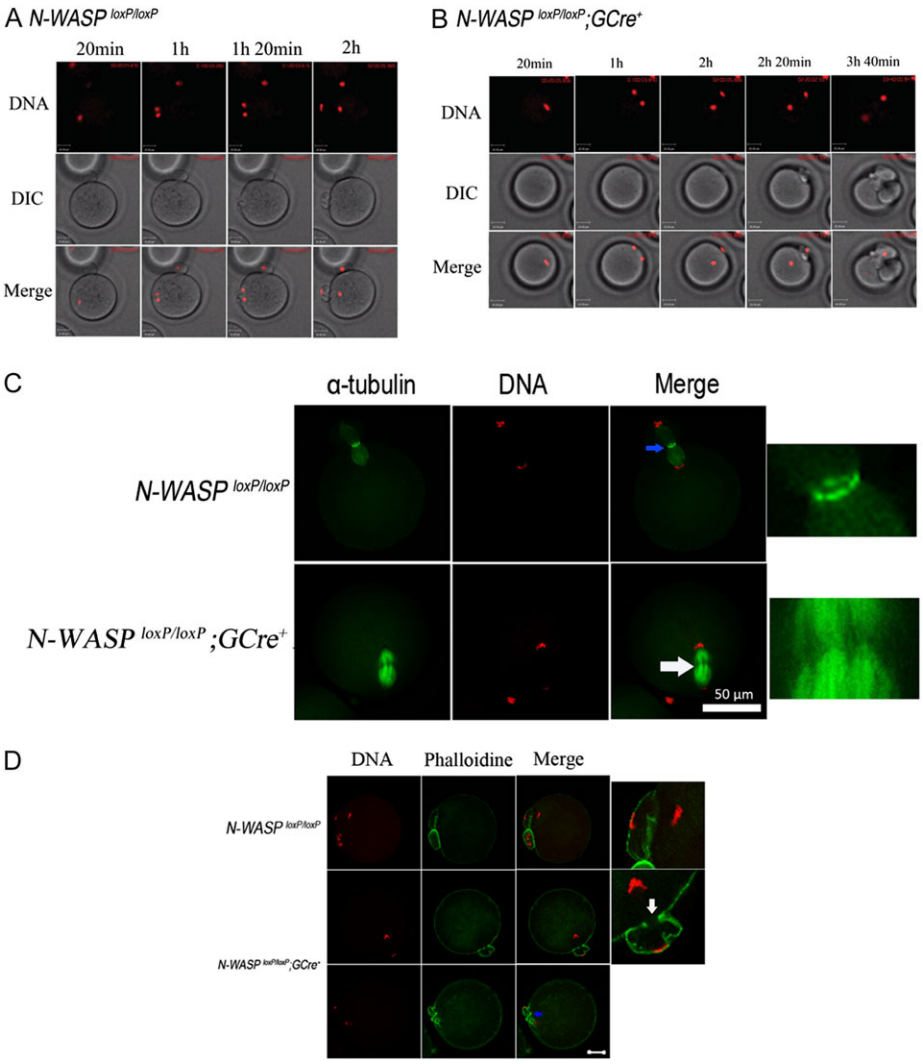

Figure 7 *N-WASP* deletion causes cytokinesis failure during meiosis II. For A and B, chromosomes were stained in blue by Hoechst 33342 [2 ng/ml in KSOM medium (Ca^{2+}, Mg^{2+} free)] and the color was changed into red. Bar = 20 μM for all images. (**A**) Dynamics of chromosomes during *N-WASP*$^{loxP/loxP}$ MII oocyte parthenogenetic activation. (**B**) Dynamics of chromosomes during *N-WASP*$^{loxP/loxP}$; *GCre*$^{+}$ MII oocyte parthenogenetic activation. (**C**) Disrupted midbody formation in anaphase II during *N-WASP*$^{loxP/loxP}$; *GCre*$^{+}$ MII oocyte parthenogenetic activation (×10). Blue arrow indicates the midbody in anaphase II during *N-WASP*$^{loxP/loxP}$ MII oocyte parthenogenetic activation. White arrow indicates no midbody in anaphase II during *N-WASP*$^{loxP/loxP}$; *GCre*$^{+}$ MII oocyte parthenogenetic activation. Green, α-tubulin; Red, DNA. Bar = 50 μm for all images except the zoom. (**D**) Impaired contractile ring in anaphase II during *N-WASP*$^{loxP/loxP}$; *GCre*$^{+}$ MII oocyte parthenogenetic activation. White arrow, indicates the gap in the contractile ring in *N-WASP*$^{loxP/loxP}$; *GCre*$^{+}$ MII oocytes. Blue arrow indicates the severely disrupted second polar body emission. Green, Alexa 488-phalloidine; Red, DNA. Bar = 20 μm for all images except the zoom.

WASP to function within the pathway for polarity establishment and maintenance in mouse oocytes. Considering that only WASP and N-WASP among the type I NPFs have the GTPase-binding domain and WASP is expressed exclusively in hematopoietic cells (Takenawa and Miki, 2001), another possibility exists. It is worth noting that the type II NPF also has acidic domains at the amino terminus that bind the ARP2/3 complex and tandem repeat domains that bind F-actin, although lack complete VCA domains, and cortactin is a member of the type II NPF. Knockout of cortactin results in disruption of the actin cap and inhibition of second polar body emission in MII oocytes (Yu *et al.*, 2010). Cortactin might be the redundant player for the polarity formation and maintenance when *N-WASP* was deleted, though the direct relationship between Cdc42 and cortactin is still lacking.

N-WASP is involved in cytokinesis during second meiosis

It appears that both *N-WASP*-deleted and control MII oocytes show normal polarity and normal asymmetric localization of the MII spindle. Through parthenogenetic activation experiments, we showed that the *N-WASP*-deleted MII oocytes could not emit the second polar body as a result of cytokinesis failure. During cell division, the midbody, as remnant of the spindle, directs cytokinesis initiation and finally forms the two daughter cells. As shown in Fig. 7C, the midbody is normal in the *N-WASP*$^{loxP/loxP}$ MII oocytes undergoing anaphase, while the midbody formation is compromised in *N-WASP*-deleted oocytes although the MII spindle is well-organized, consistent with the existence of the defect in the contractile ring (Fig. 7D). Considering that *N-WASP* deletion has no effect on spindle formation as well as cytokinesis during the first meiosis (oocyte maturation), some differences may exist in the midbody-mediated cytokinesis between the two meioses. Different mechanisms may underlie the MI and MII spindle organization in mouse oocytes. Though a RanGTP gradient has been established during meiosis I in mouse oocytes, it is not required for MI spindle organization, but it is pivotal for MII spindle formation. N-WASP deletion has no effect on both MI and MII spindle organization, while N-WASP functions in spindle separation and cytokinesis completion during meiosis II. Interestingly, *N-WASP*$^{loxP/loxP}$ deletion results in the failed constriction of the contractile ring with an obvious gap, which might be caused directly or indirectly by the impaired midbody. Taken together, N-WASP may play an important role in mediating and coordinating the activity of the spindle (midbody) and actin (contractile ring constriction) when cell division occurs.

Supplementary data

Supplementary data are available at http://molehr.oxfordjournals.org/.

Acknowledgements

We thank Dr Heng-Yu Fan (Life Science Institute, Zhejiang University, China) for providing *GDF9-Cre* transgenic mice. We are grateful for technical assistance from Dr Lijuan Wang.

Authors' roles

Conception and design: Z.-B.W., S.B.S., Q.-Y.S. Execution: Z.-B.W., X.-S.M., M.-W.H., Z.-Z.J., T.-G.M., M.-Z.D., L.-H.F., Y.-C.O. Interpretation of the data: Z.-B.W., Q.-Y.S. Preparing the article: Z.-B.W., H.S., Q.-Y.S.

Funding

The National Basic Research Program of China (No. 2012CB944404) and the National Natural Science Foundation of China (Nos 30930065, 31371451, 31272260 and 31530049).

Conflict of interest

None declared.

References

Azoury J, Lee KW, Georget V, Rassinier P, Leader B, Verlhac MH. Spindle positioning in mouse oocytes relies on a dynamic meshwork of actin filaments. *Curr Biol* 2008;**18**:1514–9.

Beaty BT, Condeelis J. Digging a little deeper: the stages of invadopodium formation and maturation. *Eur J Cell Biol* 2014;**93**:438–44.

Cotta-de-Almeida V, Westerberg L, Maillard MH, Onaldi D, Wachtel H, Meelu P, Chung UI, Xavier R, Alt FW, Snapper SB. Wiskott Aldrich syndrome protein (WASP) and N-WASP are critical for T cell development. *Proc Natl Acad Sci USA* 2007;**104**:15424–9.

Dehapiot B, Carriere V, Carroll J, Halet G. Polarized Cdc42 activation promotes polar body protrusion and asymmetric division in mouse oocytes. *Dev Biol* 2013;**377**:202–12.

Dumont J, Million K, Sunderland K, Rassinier P, Lim H, Leader B, Verlhac MH. Formin-2 is required for spindle migration and for the late steps of cytokinesis in mouse oocytes. *Dev Biol* 2007;**301**:254–65.

Gasman S, Chasserot-Golaz S, Malacombe M, Way M, Bader MF. Regulated exocytosis in neuroendocrine cells: a role for subplasmalemmal Cdc42/N-WASP-induced actin filaments. *Mol Biol Cell* 2004;**15**:520–31.

Higgs HN, Pollard TD. Regulation of actin polymerization by Arp2/3 complex and WASp/Scar proteins. *J Biol Chem* 1999;**274**:32531–4.

Higgs HN, Pollard TD. Regulation of actin filament network formation through ARP2/3 complex: activation by a diverse array of proteins. *Annu Rev Biochem* 2001;**70**:649–76.

Hu MW, Wang ZB, Jiang ZZ, Qi ST, Huang L, Liang QX, Schatten H, Sun QY. Scaffold subunit Aalpha of PP2A is essential for female meiosis and fertility in mice. *Biol Reprod* 2014;**91**:19.

Jiang ZZ, Hu MW, Wang ZB, Huang L, Lin F, Qi ST, Ouyang YC, Fan HY, Schatten H, Mak TW *et al*. Survivin is essential for fertile egg production and female fertility in mice. *Cell Death Dis* 2014;**5**:e1154.

Leader B, Lim H, Carabatsos MJ, Harrington A, Ecsedy J, Pellman D, Maas R, Leder P. Formin-2, polyploidy, hypofertility and positioning of the meiotic spindle in mouse oocytes. *Nat Cell Biol* 2002;**4**:921–8.

Ma C, Benink HA, Cheng D, Montplaisir V, Wang L, Xi Y, Zheng PP, Bement WM, Liu XJ. Cdc42 activation couples spindle positioning to first polar body formation in oocyte maturation. *Curr Biol* 2006;**16**:214–20.

Martinez-Quiles N, Rohatgi R, Anton IM, Medina M, Saville SP, Miki H, Yamaguchi H, Takenawa T, Hartwig JH, Geha RS *et al*. WIP regulates N-WASP-mediated actin polymerization and filopodium formation. *Nat Cell Biol* 2001;**3**:484–91.

Miki H, Miura K, Takenawa T. N-WASP, a novel actin-depolymerizing protein, regulates the cortical cytoskeletal rearrangement in a PIP2-dependent manner downstream of tyrosine kinases. *EMBO J* 1996;**15**:5326–35.

Nakagawa H, Miki H, Ito M, Ohashi K, Takenawa T, Miyamoto S. N-WASP, WAVE and Mena play different roles in the organization of actin cytoskeleton in lamellipodia. *J Cell Sci* 2001;**114**:1555–65.

Padrick SB, Rosen MK. Physical mechanisms of signal integration by WASP family proteins. *Annu Rev Biochem* 2010;**79**:707–35.

Pfender S, Kuznetsov V, Pleiser S, Kerkhoff E, Schuh M. Spire-type actin nucleators cooperate with Formin-2 to drive asymmetric oocyte division. *Curr Biol* 2011;**21**:955–60.

Pollard TD, Beltzner CC. Structure and function of the Arp2/3 complex. *Curr Opin Struct Biol* 2002;**12**:768–74.

Qiao J, Wang ZB, Feng HL, Miao YL, Wang Q, Yu Y, Wei YC, Yan J, Wang WH, Shen W *et al*. The root of reduced fertility in aged women and possible therapentic options: current status and future perspects. *Mol Aspects Med* 2014;**38**:54–85.

Rocca DL, Hanley JG. PICK1 links AMPA receptor stimulation to Cdc42. *Neurosci Lett* 2015;**585**:155–9.

Rotty JD, Wu C, Bear JE. New insights into the regulation and cellular functions of the ARP2/3 complex. *Nat Rev Mol Cell Biol* 2013;**14**:7–12.

Sun SC, Wang ZB, Xu YN, Lee SE, Cui XS, Kim NH. Arp2/3 complex regulates asymmetric division and cytokinesis in mouse oocytes. *PLoS One* 2011;**6**:e18392.

Takenawa T, Miki H. WASP and WAVE family proteins: key molecules for rapid rearrangement of cortical actin filaments and cell movement. *J Cell Sci* 2001;**114**:1801–9.

Verlhac MH, Lefebvre C, Guillaud P, Rassinier P, Maro B. Asymmetric division in mouse oocytes: with or without Mos. *Curr Biol* 2000;**10**:1303–6.

Wang L, Wang ZB, Zhang X, FitzHarris G, Baltz JM, Sun QY, Liu XJ. Brefeldin A disrupts asymmetric spindle positioning in mouse oocytes. *Dev Biol* 2008;**313**:155–66.

Wang ZB, Jiang ZZ, Zhang QH, Hu MW, Huang L, Ou XH, Guo L, Ouyang YC, Hou Y, Brakebusch C *et al*. Specific deletion of Cdc42 does not affect meiotic spindle organization/migration and homologous chromosome segregation but disrupts polarity establishment and cytokinesis in mouse oocytes. *Mol Biol Cell* 2013;**24**:3832–41.

Wang ZB, Ou XH, Tong JS, Li S, Wei L, Ouyang YC, Hou Y, Schatten H, Sun QY. The SUMO pathway functions in mouse oocyte maturation. *Cell Cycle* 2010;**9**:2640–6.

Wang ZB, Schatten H, Sun QY. Why is chromosome segregation error in oocytes increased with maternal aging?. *Physiology (Bethesda)* 2011;**26**:314–25.

Wegner AM, Nebhan CA, Hu L, Majumdar D, Meier KM, Weaver AM, Webb DJ. N-wasp and the arp2/3 complex are critical regulators of actin in the development of dendritic spines and synapses. *J Biol Chem* 2008;**283**:15912–20.

Yamaguchi H, Lorenz M, Kempiak S, Sarmiento C, Coniglio S, Symons M, Segall J, Eddy R, Miki H, Takenawa T *et al*. Molecular mechanisms of invadopodium formation: the role of the N-WASP-Arp2/3 complex pathway and cofilin. *J Cell Biol* 2005;**168**:441–52.

Yi K, Rubinstein B, Unruh JR, Guo F, Slaughter BD, Li R. Sequential actin-based pushing forces drive meiosis I chromosome migration and symmetry breaking in oocytes. *J Cell Biol* 2013;**200**:567–76.

Yi K, Unruh JR, Deng M, Slaughter BD, Rubinstein B, Li R. Dynamic maintenance of asymmetric meiotic spindle position through Arp2/3-complex-driven cytoplasmic streaming in mouse oocytes. *Nat Cell Biol* 2011;**13**:1252–8.

Yu D, Zhang H, Blanpied TA, Smith E, Zhan X. Cortactin is implicated in murine zygotic development. *Exp Cell Res* 2010;**316**:848–58.